A Model for the Passivation of the Zinc Electrode in Alkaline Electrolyte

Geoffrey Prentice,* Yu-Chi Chang,*,[1] and Xuning Shan

Department of Chemical Engineering, The Johns Hopkins University, Baltimore, Maryland 21218

ABSTRACT

We have developed a model for the anodic dissolution and passivation of the zinc electrode in alkaline electrolyte. The model is based on postulated elementary reactions. Species on the electrode surface are assumed to follow Langmuir behavior. In previous work we proposed a model for the dissolution kinetics in the prepassive region. In the present investigation we have extended this model to include the passivation process. Using our model, we are able to simulate the general features of the current-potential behavior. Effects of hydroxide concentration and mass transport rates on current-potential curves are qualitatively predicted by the model.

We have been developing a model for the kinetics and mechanism of anodic zinc dissolution in alkaline electrolyte (1-4). In previous work we postulated reactions that were assumed to dominate in the prepassive region, from the rest potential to the passivation potential. Partially soluble species were assumed to form monolayers on the electrode surface, and these were modeled using a Langmuir treatment. From ellipsometric and coulometric measurements, we showed that the film was several hundred ångströms thick in the passive region (5). Thinner films detected in the prepassive region were consistent with our use of the monolayer model in that potential region.

The kinetic model developed in the initial dissolution region was similar to the model presented by Bockris *et al.* (6). In the prepassive region we demonstrated agreement with observed experimental quantities such as current-potential behavior and reaction order. In the present work we show that the introduction of a relatively insoluble ZnO species can account for electrode passivation. The rapidity of the passivation process can be attributed to an essentially reversible reaction that leads to the formation of ZnO or other oxides.

Experimental

Rotating disk experiments were carried out on a Pine Instrument ASR rotator with the Model AFDTI36 disk assembly and an RDE 3 potentiostat. Zinc disks 0.5 cm diam and 99.99% pure were used. Potential was measured with respect to a custom-built Hg/HgO reference electrode. Temperature was controlled to 0.1°C by a Thermomix 1480 thermostat. The working electrode compartment was custom-built from a 3 liter Teflon beaker. A separate compartment was built for the platinum counterelectrode, which was connected to the working electrode compartment through a Teflon U-tube. All electrolyte solutions were prepared from analytical grade chemicals and 10 MΩ-cm deionized water. No zincates were initially present. The solutions were sparged with nitrogen prior to use, and a nitrogen blanket was maintained throughout the experiment.

Model System

Our model is based on postulated elementary reactions with surface coverage of reacting species being treated by a Langmuir model. A list of potential reactions is summarized by Valdes *et al.* (7). In the initial dissolution region the following reactions are considered to be of greatest importance (1)

$$Zn + OH^- = ZnOH + e \quad [1]$$

$$ZnOH + 2\,OH^- = Zn(OH)_3^- + e \text{ rds} \quad [2]$$

$$Zn(OH)_3^- + OH^- = Zn(OH)_4^{2-} \quad [3]$$

where rds indicates rate-determining step. At more positive potentials, we postulate that the following reaction path (4) leads to the formation of a less soluble film of zinc hydroxide [$Zn(OH)_2$]. Film formation reduces the current from levels that would occur if only the first three reactions were dominant

$$ZnOH + OH^- = Zn(OH)_2 + e \quad [4]$$

$$Zn(OH)_2 + OH^- = Zn(OH)_3^- \text{ rds} \quad [5]$$

We assume that passivation is caused by the presence of zinc oxide and peroxide formed in the following steps

$$Zn + Zn(OH)_2 + 2\,OH^- = Zn(OH)_3^- + ZnOH + e \text{ rds} \quad [6]$$

$$Zn + Zn(OH)_2 + (2 + 2Y)OH^- = (2 - Y)ZnO + (2 + Y)H_2O + YZnO_2 + (2 + 2Y)e \quad [7]$$

Reaction [7] indicates that a combination of oxides and peroxides may be formed. More generally, nonstoichiometric compounds could be formed in similar reaction schemes. Reaction [7] requires the transfer of multiple electrons and cannot be considered to be an elementary reaction. Evidence for the existence of the peroxide ZnO_2 is indicated in references with the Pourbaix diagram and in the work of Popova *et al.* (8). The model is also valid in the absence of peroxides. For $Y = 0$, reaction [7] becomes

$$Zn + Zn(OH)_2 + 2\,OH^- = 2ZnO + 2H_2O + 2e \quad [8]$$

Because the overall process of oxide and peroxide formation is considered to be essentially an equilibrium process, the details are of minor importance in the kinetic model. From reaction [7] we can evaluate the thermodynamics and the shifts in reversible potential due to changes in temperature and local composition. The oxides are soluble in alkaline electrolyte, resulting in a finite current in the passive region. This process appears to be a straightforward dissolution, but we have not yet incorporated it in our model.

Analysis of Rate Expressions

The rate-determining steps are assumed to control the overall reaction rate. In the remaining steps, we assume that the reactions are fast and the species are essentially at equilibrium. The overall rate is the sum of the rates of the parallel paths

$$r = r_2 + r_5 + r_6 \quad [9]$$

In this analysis we treat each of the three paths as independent. A reactant in one path may be a product from another path. For example, the reactant ZnOH in reaction [4] is formed in reaction [1]. Two electrons (one from reaction [1] and one from reaction [2]) are transferred in the formation of $Zn(OH)_3^-$ through reaction [5]. The overall rate can be expressed in terms of the current densities for those reactions involving charge transfer

$$i = 2i_2 + 2\mathbf{F}r_5 + 3i_6 \quad [10]$$

*Electrochemical Society Active Member.
[1]Present address: Tamkang University, Tamsui, Taiwan.

Oxides and hydroxides are assumed to exist on active sites: θ_1 is ZnOH, θ_2 is $Zn(OH)_2$, and θ_3 is ZnO and ZnO_2. Equation [10] can be expressed in terms of elementary rate equations as the net current for the reactions as written

$$2i_2 = 2\mathbf{F}k_{f2}\theta_1 c^2_{OH^-} \exp(\beta_2 \mathbf{F}V/RT) - 2\mathbf{F}k_{r5}(1 - \theta_1 - \theta_2 - \theta_3) \exp[-(1 - \beta_2)\mathbf{F}V/RT]c_{z3} \quad [11]$$

$$2\mathbf{F}r_5 = 2\mathbf{F}k_{f5}\theta_2 c_{OH^-} - 2\mathbf{F}k_{r5}c_{z3} \quad [12]$$

$$3i_6 = 3\mathbf{F}k_{f6}\theta_2 c^2_{OH^-} \exp(\beta_6 \mathbf{F}V/RT) - 3\mathbf{F}k_{r6} \exp[-(1 - \beta_6)\mathbf{F}V/RT]\theta_1 c_{z3} \quad [13]$$

where the ks are kinetic constants, $1 - \beta$ terms are symmetry factors, and V is the potential. The subscript f refers to the forward reaction, r refers to the reverse reaction, and $z3$ is $Zn(OH)_3^-$. The fractional surface coverage can be expressed in terms of the equilibrium constants Ks for those reactions considered to be at equilibrium

$$\theta_1 = K_1(1 - \theta_1 - \theta_2 - \theta_3) C_{OH^-} \exp(\mathbf{F}V/RT) \quad [14]$$

$$\theta_2 = K_4 C_{OH^-}\theta_1 \exp(\mathbf{F}V/RT) \quad [15]$$

$$\theta_3 = K_7 C_{OH^-}\theta_2 \exp[(2 + 2Y)\mathbf{F}V/RT] \quad [16]$$

We indicate the hydroxide concentration to be in molar units by C_{OH^-} (uppercase) in the equilibrium expressions; these units are consistent with usual choice of units for standard state concentration. By contrast, the hydroxide concentration in the rate expressions (Eq. [11]-[13]) is expressed in units of mol/cm^3 and indicated in lowercase.

The above expressions for fractional surface coverage can be solved simultaneously to obtain explicit expressions for the θ

$$\theta_1 = K_1 C_{OH^-} \exp(\mathbf{F}V/RT)/Q \quad [17]$$

$$\theta_2 = K_1 K_4 C^2_{OH^-} \exp(2\mathbf{F}V/RT)/Q \quad [18]$$

$$\theta_3 = K_1 K_4 K_7 C^{(4+2Y)}_{OH^-} \exp[(4 + 2Y)\mathbf{F}V/RT]/Q \quad [19]$$

where

$$Q = 1 + K_1 C_{OH^-} \exp(\mathbf{F}V/RT) + K_1 K_4 C^2_{OH^-} \exp(2\mathbf{F}V/RT) + K_1 K_4 K_7 C^{(4+2Y)}_{OH^-} \exp[(4 + 2Y)\mathbf{F}V/RT] \quad [20]$$

The three rate expressions (Eq. [11]-[13]) along with the three equilibrium expressions for the surface coverage (Eq. [17]-[19]) provide a description of the current-potential behavior in a kinetically limited system.

To compare the simulated results with experimental data, we need to consider mass transport effects. Because our experiments were conducted on a rotating disk electrode, we estimated the surface concentration of hydroxide ion through the Levich equation

$$i_l = A c_b \omega^{1/2} \quad [21]$$

where

$$A = 0.62n\mathbf{F}D^{2/3}\nu^{-1/6} \quad [22]$$

We also assumed that the surface hydroxide concentration decreased in proportion to the current density

$$\frac{i}{i_l} = 1 - \frac{c_o}{c_b} \quad [23]$$

or

$$c_o = c_b - \frac{i}{A\omega^{1/2}} \quad [24]$$

Because the zinc disk is dissolving and because there is partial surface coverage of the disk, this estimate of the hydroxide concentration is only approximate.

As mentioned above, the kinetically limited case can be determined explicitly by substituting Eq. [17]-[19] into Eq. [11]-[13], which are summed according to Eq. [10]. When mass transport is taken into account, the current density and the hydroxide concentration are coupled through Eq. [24]. As a consequence, an iterative solution is required.

We solved these equations by first computing the kinetically limited current density, then substituting this current density into Eq. [24] and calculating the concentration of hydroxide at the surface. A new estimate of the current density was calculated with the revised hydroxide concentration. These steps were repeated until the current density changed by less than a percent between iterations. As we stepped through the potential range, the hydroxide concentration from the previous potential served as the initial estimate at the new potential.

Results and Discussion

To carry out the simulation, we need to supply kinetic and thermodynamic parameters: k, K, Y, and β. In addition, we need values for transport properties, ν and D. We used the Davies equation (9) to estimate an activity coefficient for hydroxide ions. At 1N KOH the activity coefficient was 0.76.

For most of the thermodynamic parameters, values are obtainable from the literature. Molar free energies of formation and entropies of formation [Ref. (10) and (11)] for each species are listed in Table I.

Kinetic constants for these elementary reactions have not been determined, but they can be chosen to fit the experimental current-potential curves. Values of the symmetry factors are often near 0.5, and we chose this value for all cases. We chose $Y = 1$ and $Y = 0$ in different simulations, representing varying mixtures of oxides and peroxides.

The concentration of $Zn(OH)_3^-$ at the electrode surface was not readily estimated, but because it enters into a reversible reaction that favors the product side (reaction [3]), its concentration should generally be small. We chose a constant value for the $Zn(OH)_3^-$ concentration of 10^{-10} mol/cm^3.

As a base case we considered the anodic polarization of the zinc electrode in 1N KOH. To compare simulated results with experimental data we obtained current-potential curves on a rotating disk electrode. For the base case we used 1200 rpm and 25°C.

When we attempted to fit the experimental current-potential curve by adjusting only the kinetic constants in the rate-determining steps, we were able to replicate the general features of the curve. When we chose $Y = 0$ (only ZnO in the passivating film), the simulated passivation potential was 350 mV more negative than the experimental value. In our model, passivation is caused by the formation of oxides and peroxides in a reversible reaction (reaction [7]).

This discrepancy between calculated and experimental passivation potentials led us to consider two possible explanations: (*i*) changes in local pH leading to changes in reversible potential of reaction [7] or (*ii*) the presence of other reacting species with different free energies of formation. Because the current density is high just prior to passivation, the hydroxide concentration at the disk surface is lower than the bulk concentration. Partial electrode coverage by a film makes the local pH difficult to determine. From a model we developed (3), we showed that a surface film could lower the pH and shift the reversible potential of reaction [7] in a positive direction. For reaction [7] a posi-

Table I. Molar free energies of formation and entropies of formation for species used in the simulation. All values from the literature except for ZnOH, which was estimated.

Species	ΔG°_f (kJ)	ΔS°_f (J/K)
H_2O	−237	69.9
OH^- (m = 1)	−157	−10.8
Zn	0	41.7
ZnOH	−276	—
$Zn(OH)_2$	−557	81.6
ZnO	−319	43.5
$Zn(OH)_3^-$ (m = 1)	−695	—
$Zn(OH)_4^{2-}$ (m = 1)	−157	—

Table II. Kinetic and transport parameters used in the base case simulation.

Quantity	Value
k_{f2}	2×10^9 cm^4/(s mol)
k_{f5}	5.2×10^{-4} cm/s
k_{f6}	1.8×10^7 cm^4/(s mol)
β (all)	0.5
Y	1
D_{OH^-}	1×10^{-5} cm^2/s
ν	1×10^{-2} cm^2/s
ω	126 rad/s (1200 rpm)
T	298 K
C_{OH^-}	1N
C_{z3}	1×10^{-10} mol/cm^3

tive shift in reversible potential with hydroxide concentration of 60 mV/decade can be estimated from the Nernst equation. The second possibility can be characterized by values of $Y > 0$. For example, if we choose $Y = 1$ and $\Delta G_f^\circ = -500$ kJ for ZnO_2, the reversible potential for reaction [7] agrees with the experimental passivation potential. Either modification (or a combination of both) can account for the shift in reversible potential.

Values of kinetic and transport parameters for the base case simulation are listed in Table II. Free energy changes of reaction used in the simulation were approximately the same as those calculated from the literature, except for the free energy change of reaction [7], as noted above. A comparison of the thermodynamic parameters used with those calculated from literature values is shown in Table III. Thermodynamic values used in reaction [1] were calculated from an estimated value of ΔG_f° for ZnOH; consequently, the calculated thermodynamic values and those used in the simulation for reaction [1] agree. Thermodynamic values for reaction [7] in Table III were calculated with the base case value of $Y = 1$. In the reaction labeled [7a], we used $Y = 0$, representing all ZnO.

Comparison between simulated and experimental polarization curves appear in Fig. 1. The general features of the experimental curve are present in the simulated curve, and the current densities agree within about 10 mA/cm^2 at all potentials. Contributions to the total current density from individual reactions are shown in Fig. 2. Electrode coverage by partially soluble species was calculated from Eq. [17]-[19]. A plot of fractional coverage *vs.* potential appears in Fig. 3.

We performed a number of simulations to test the sensitivity of the model. We recognized that the use of the Levich equation in the calculation of hydroxide concentration was approximate. Simulations with rotation rates of 300 and 3000 rpm were calculated and compared with the base case (Fig. 4). As expected, higher rotation rates increase the local hydroxide concentration and increase the maximum current density. A comparison of the polarization curve with the simulation at 2400 rpm reveals that the increase in maximum current density from the simulated curve is much too low (Fig. 5). Even at infinite rotation rate, the maximum simulated current density is less than 130 mA/cm^2.

If we make the assumption that the kinetic constants are concentration dependent, we can adjust them in an attempt to improve the agreement. We also note that the experimental passivation potential shifts slightly in a positive direction. We might assume that the surface pH is further lowered by the increased current density in the pre-passive region. In accordance with the Nernst equation, the reduced pH would further increase the reversible potential of reaction [7]. An increase of k_{f2} by 50% and k_{f5} by 80% gives a better fit of the polarization curves. The sensitivity of the simulated curves to these changes is shown in Fig. 6. A change in the logarithm of the equilibrium constant K_7 by 4% is also shown. The fit could undoubtedly be improved by adjusting other parameters in a manner consistent with physical principles.

We checked the assumption of using a small concentration of $Zn(OH)_3^-$. Increasing or decreasing the concentration of $Zn(OH)_3^-$ by an order of magnitude has little effect on the simulated curves. Over this concentration range the current density changes by less than 10 mA/cm^2 at any potential.

We have not yet attempted to make quantitative comparisons between simulated and experimental results at

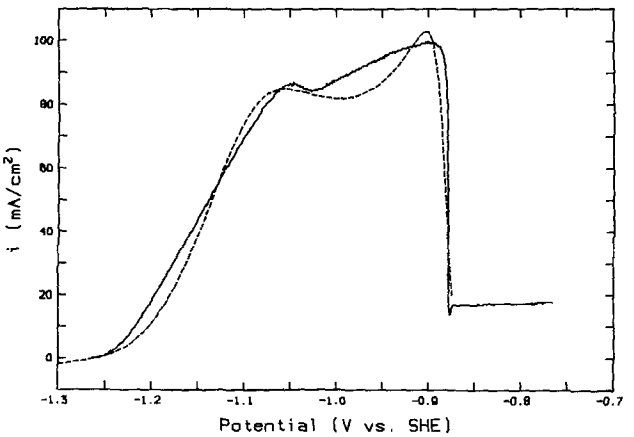

Fig. 1. Current density vs. potential for a zinc electrode in alkaline electrolyte. Base case conditions are specified in Table II. Solid line represents experimental values and dashed line is simulated result.

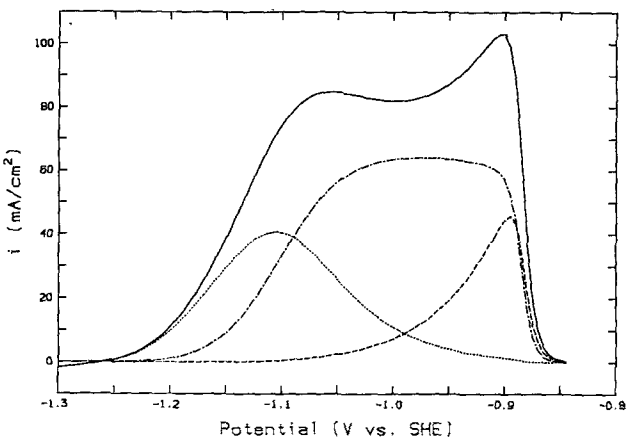

Fig. 2. Simulated current density vs. potential for the base case (Table II). Solid line is total current density, dotted line is $2i_2$, dashed-dotted line is current from reaction [5], and dashed line is $3i_6$.

Table III. Comparison of calculated standard thermodynamic values with those used in the simulation. Reaction [7a] represents reaction [7] with $Y = 0$.

Reaction	ΔG_r° (kJ)		ln K		E° (V)	
	(calc.)	(used)	(calc.)	(used)	(calc.)	(used)
1	−118	−118	47.7	47.7	−1.22	−1.22
2	−105	−104	42.3	42.0	−1.08	−1.08
3	−5.86	−7.03	2.37	2.84	—	—
4	−124	−107	50.0	43.3	−1.28	−1.11
5	19.3	17.8	−7.77	−7.17	—	—
6	−98.8	−100	39.9	40.6	−1.02	−1.04
7	−346	−346	140	140	−0.896	−0.896
7a	−240	−171	97.0	69.2	−1.24	−0.896

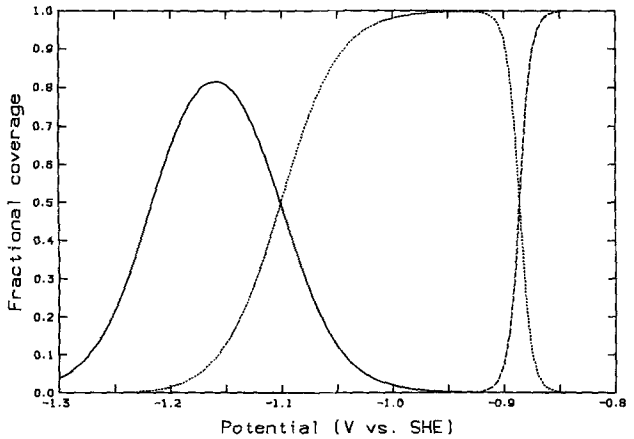

Fig. 3. Fractional surface coverage of the electrode *vs.* potential for the base case (Table II). Solid line is ZnOH, dotted line is $Zn(OH)_2$, and dashed line is ZnO and ZnO_2.

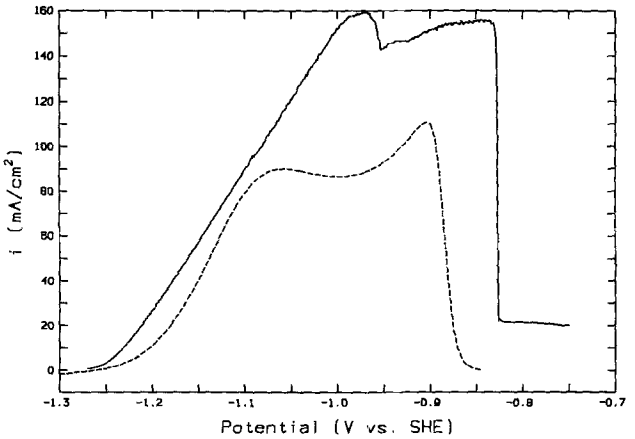

Fig. 5. Comparison of experimental (solid line) and simulated (dashed line) polarization curves. All conditions as in the base case (Table II) except 2400 rpm rotation rate.

higher temperatures and hydroxide concentrations; however, we can make several qualitative observations. From previous studies (12) we know that the maximum current density and passivation potential both increase with increasing hydroxide concentration (near 1*M* KOH) and temperature (near room temperature). Increasing the bulk hydroxide concentration is qualitatively similar to increasing the rotation rate in that both effects tend to increase maximum current and passivation potential. As we demonstrated, our model is consistent with these qualitative trends with respect to rotation rate.

We can estimate the change in reversible potential with temperature for reaction [7] from the thermodynamic relationship

$$\left(\frac{\partial E}{\partial T}\right)_p = \frac{\Delta S}{n\mathbf{F}} \qquad [25]$$

For reaction [7] with $Y = 0$, the entropy change of reaction calculated from the data in Table I is −81.6 J/K for the reduction reaction. From Eq. [25] this entropy change corresponds to −0.4 mV/K. Near room temperature the passivation potential increases by about 10 mV/K. The calculated change in reversible potential is opposite to that observed, and the magnitude of the change in relatively small; therefore, the variation in reversible potential with temperature cannot be attributed to entropy effects. An alternate explanation, consistent with our model, is that the increased maximum current density at higher temperatures reduces the near-surface pH sufficiently to shift the reversible potential of reaction [7] in a more positive direction.

From the model and data, we can describe a plausible series of steps that explain the general features of the current density-potential curves. Near the rest potential a thin, reactive film of ZnOH partially covers the electrode, and current density increases rapidly with potential. At intermediate potentials the current density becomes moderated by the influence of a slower chemical dissolution of $Zn(OH)_2$. At higher potentials the electrode passivates through the formation of oxides and peroxides in rapid reactions. In the passive region the current density drops by about an order of magnitude. Current in this region is limited by the chemical dissolution of oxides and peroxides.

Increased temperature, hydroxide concentration, and rotation rate all increase the maximum current density when these parameters are maintained in a region near our base case. The passivation potential increases with increasing maximum current density. We can offer a plausible explanation for these phenomena. The higher maximum rate, owing to higher hydroxide concentration and larger rate constants, can be maintained until islands of oxides begin to form and partially block a portion of the electrode surface. Oxide blocking increases local current density on the unblocked portion of the electrode. Higher current density just prior to passivation reduces the near-surface pH. The lower pH, in turn, shifts the reversible potential of the passivating reactions to more positive potentials.

The monolayer surface coverage approximation becomes poorer near the passivation potential, and film thickening in this region may also contribute to lower pH. Our measurements show that increased rotation rate, hydroxide concentration and temperature are all factors that lead to thicker passive films (5). Although we were not able

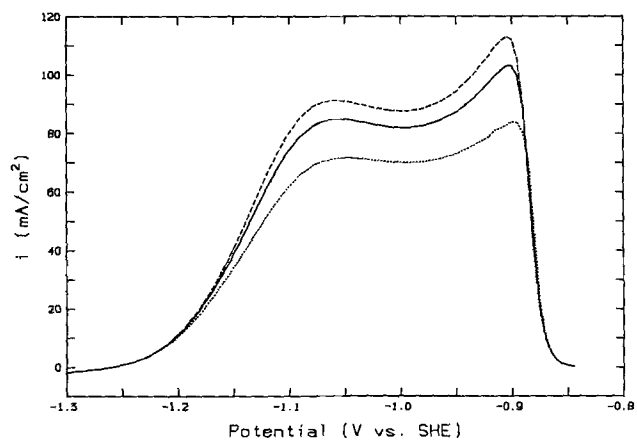

Fig. 4. Effect of rotation rate on the simulated current density *vs.* potential curves. Solid line is 1200 rpm (base case, Table II), dashed line is 3000 rpm, and dotted line is 300 rpm.

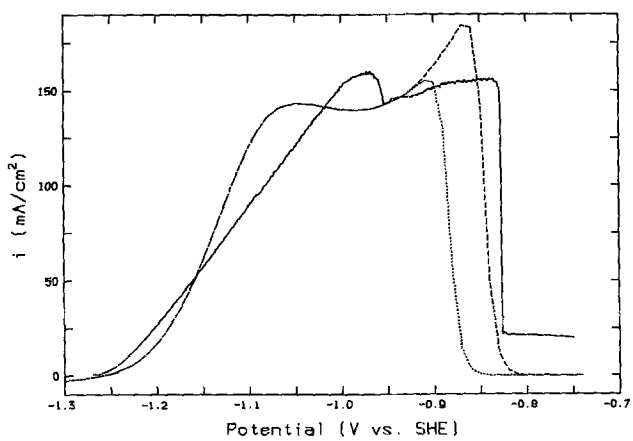

Fig. 6. Comparison of experimental polarization curve (solid line) with simulated curves. Dotted line represents simulation with adjustment of kinetic parameters [$k_{f2} = 3 \times 10^9$ cm⁴/(s mol), $k_{f5} = 5 \times 10^{-4}$ cm/s]. Dashed line represents the same adjusted kinetic parameters and ln $K_7 = 134$.

to measure the thickness of the film on rotating electrodes just prior to passivation, we speculate that these same factors (rotation rate, hydroxide concentration, and temperature) also increase the thickness of the pre-passive film.

The simulation (Fig. 3) indicates that the growth of islands occurs over a small potential range; oxide coverage increases from 7 to 95% over a 30 mV range. This potential sensitivity could also contribute to the oscillatory current behavior observed just prior to passivation (13).

Further evidence for this passivation mechanism can be seen in the simulation of Fig. 6 (dashed line). When we use the base-case value for k_{f6}, we see that the simulated current density just prior to passivation is too large. If we use a lower value for the hydroxide concentration due to partial electrode blocking, then reaction [6] would proceed more slowly. The lower current density just prior to passivation would be closer to the observed value.

Conclusions

The proposed model for the dissolution kinetics and passivation mechanism of zinc in alkaline electrolyte is consistent with observed current-potential behavior. In previous work we demonstrated that experimentally determined quantities such as Tafel slope and reaction orders were also consistent with the model. The increase in maximum current density with increased rotation rate on a rotating disk electrode can only be partially explained by an increase in mass-transfer rate; quantitative agreement can only be obtained when kinetic rate constants are assumed to be a function of local hydroxide concentration. We must also assume either that near-surface pH changes affect the reversible potential of the passivating reaction or that a mixture of oxides and peroxides is present in the passivating film. Although our model is based on a direct-reaction mechanism for electrode passivation, other mechanisms may also be consistent. We are currently conducting radiotracer studies to discriminate among several proposed passivation mechanisms.

Acknowledgment

This material is based upon work supported by the National Science Foundation under Grant No. CBT 8611604.

Manuscript submitted Aug. 24, 1990; revised manuscript received Oct. 22, 1990.

LIST OF SYMBOLS

c	concentration, mol/cm^3
C	concentration, mol/liter
D	diffusivity, cm^2/s
E	reversible potential, V
F	Faraday's constant, 96,500 C/equiv
G	Gibbs free energy, kJ
i	current density, A/cm^2
k	kinetic rate constant, cm/s or cm^4/mol s
K	equilibrium constant
n	number of electrons
p	pressure, bar
r	reaction rate, mol/s cm^2
R	gas constant, 8.31 J/mol K
S	entropy, J/K
T	temperature, K
V	potential, V
Y	stoichiometric coefficient for ZnO_2

Greek symbols

β	symmetry factor
θ	fractional surface coverage
ν	kinematic viscosity, cm^2/s
ω	rotation rate, rad/s

Subscripts

b	bulk
f	forward
f	formation
l	limiting
o	surface
r	reverse
r	reaction
$z3$	$Zn(OH)_3^-$

Superscripts

o	standard conditions

REFERENCES

1. Y.-C. Chang and G. A. Prentice, *This Journal,* **131,** 1465 (1984).
2. Y.-C. Chang and G. A. Prentice, *ibid.,* **132,** 375 (1985).
3. Y.-C. Chang and G. A. Prentice, *Electrochim. Acta,* **31,** 579 (1986).
4. Y.-C. Chang and G. A. Prentice, *This Journal,* **136,** 3398 (1989).
5. X. Shan, D. Ren, P. Scholl, and G. A. Prentice, *ibid.,* **136,** 3594 (1989).
6. J. O'M. Bockris, Z. Nagy, and A. Damjanovich, *ibid.,* **119,** 285 (1972).
7. J. L. Valdes, C. Y. Mak, J. Happel, and H. Y. Cheh, *Chem. Eng. Commun.,* **38,** 332 (1985).
8. T. I. Popova, N. A. Simonova, and B. N. Kabanov, *Soviet Electrochem.,* **3,** 1273 (1967).
9. D. P. Boden, R. B. Wylie, and V. J. Spera, *This Journal,* **118,** 1298 (1971).
10. "Lang's Handbook of Chemistry," 12th ed., J. A. Dean, Editor, Table 9-1, McGraw-Hill, Inc., New York (1979).
11. T. P. Dirkse, in "Zinc-Silver Oxide Batteries," A. Fleischer and J. J. Lander, Editors, p. 22, John Wiley & Sons, Inc., New York (1971).
12. G. A. Prentice and Y.-C. Chang, in "Electrochemical Engineering Applications," R. E. White, R. F. Savinell, and A. Schneider, Editors, AIChE Symp. Series, **83,** 9 (1987).
13. M. C. H. McKubre and D. D. Macdonald, *This Journal,* **128,** 524 (1981).